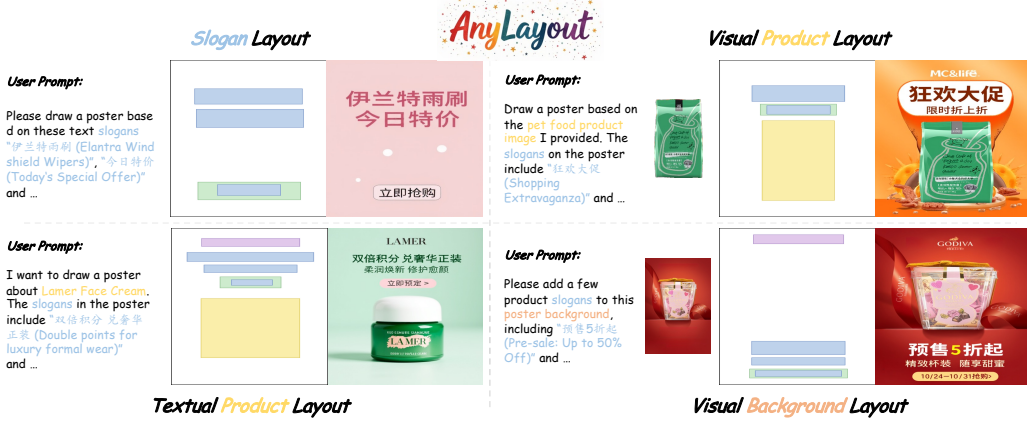


# 000 ANYLAYOUT: VERSATILE ADVERTISING POSTER 001 LAYOUT GENERATION WITH MLLMS 002

003 **Anonymous authors**

004 Paper under double-blind review



005 Figure 1: Illustration of our novel, versatile layout generation task: AnyLayout (with four subtasks).  
006

## 007 ABSTRACT

008 Layout design is a fundamental aspect of visual communication, widely used  
009 in advertising, publishing, and digital media. Recent datasets and methods, in-  
010 cluding content-agnostic and content-aware approaches, have advanced automatic  
011 layout generation, and large language models (LLMs) and multi-modal LLMs  
012 (MLLMs) have further improved performance. However, most existing methods  
013 focus on predicting bounding boxes for limited design elements on fixed back-  
014 grounds, which restricts their capability to tackle diverse instruction-driven tasks  
015 in real-world applications. To address these limitations, we introduce **AnyLayout-120K**,  
016 a large-scale instruction-driven dataset for multimodal layout generation.  
017 It offers: (1) *Task Diversity*—comprising four instruction-driven sub-tasks that  
018 encompass multimodal design elements such as multi-lingual text, visual/textual  
019 product, logos and background underlays; (2) *Rich Annotations*—including user  
020 instructions, multimodal inputs and spatial annotations; (3) *Downstream Compat-  
021 ibility*—where, in addition to the layout of individual elements, we propose com-  
022 posite layouts that capture the overall design, integrating both details and seman-  
023 tics. These composite layouts can be seamlessly incorporated into text-to-image  
024 (T2I) models for end-to-end generation. Alongside this dataset, we develop 7  
025 geometry-aware evaluation metrics that assess spatial precision and adherence to  
026 design principles, ensuring a more comprehensive evaluation. Furthermore, util-  
027 izing this dataset, we establish a strong baseline based on MLLMs, achieving  
028 state-of-the-art performance. The dataset, metrics, and baseline will be released  
029 to support future research in instruction-driven layout design.

## 030 1 INTRODUCTION

031 Layout design serves as a fundamental element of visual communication, with essential applications  
032 across various domains, including advertising, publishing, digital media, and information design  
033 (Yang et al., 2016). Advancements in this field have been marked by the development of notable  
034 datasets such as CGL and PKU (Zhou et al., 2022; Hsu et al., 2023), alongside a variety of methods

054 that encompass both content-agnostic (Li et al., 2019; Chakraborty et al., 2022; Melendez & Havas, 055 2025) and content-aware (Zheng et al., 2019; Zhang et al., 2025b; Pu et al., 2025) approaches. 056 Recently, there has been an increasing trend toward utilizing LLMs or MLLMs (Hurst et al., 2024; 057 Chu et al., 2024; Chen et al., 2025b; Lu et al., 2024) for automatic layout design (Hsu & Peng, 2025; 058 Cheng et al., 2024; Qu et al., 2025), leading to remarkable improvements in performance.

059 Despite these advancements, existing methods primarily focus on one single task: predicting bounding 060 boxes for a limited set of design elements on a given background image. Consequently, they 061 struggle to handle various user design requirements in real-world applications. For instance, user 062 instructions such as “*Given an image of a face cream product, design a poster featuring the product* 063 *on a pink background with a ‘best-seller’ slogan*” still present great challenges. Such open-ended 064 user instructions that specify multiple design elements – including product images, slogans, and 065 background specifications – highlight the necessity for more versatile layout generation.

066 In this paper, we extend the field of layout design to more flexible and practical settings, and introduce 067 **AnyLayout-120K**, a large-scale instruction-driven layout dataset. This dataset advances the 068 field through three key innovations as shown in Tab. 1: (1) **Task Diversity**. It encompasses four 069 distinct sub-tasks represented by user instructions, which incorporates multiple interleaved multi- 070 modal design elements (e.g., text, logos in two languages, and underlays). (2) **Rich Annotations**. 071 In addition to the instructions, multimodal design elements, and traditional spatial annotations (e.g., 072 bounding boxes for individual elements), it also provides structured natural language descriptions of 073 *composite* layouts — capturing both element-level details and overall design semantics. (3) **Down- 074 stream Compatibility**. The structured layout descriptions can be seamlessly integrated with T2I 075 models, facilitating end-to-end content generation. Based on this dataset, we develop an enhanced 076 evaluation system comprising 7 *geometry-aware evaluation metrics* that move past conventional 077 IoU-style scoring. These metrics quantify both spatial precision and adherence to design principles 078 (e.g., utilization, non-occlusion), thus ensuring a more comprehensive evaluation.

079 Furthermore, engaging with AnyLayout-120K presents challenges that require deep multi-modal 080 understanding: the model must effectively align visual and textual semantics, adhere geometric 081 constraints, and produce coherent and appealing layouts under diverse conditions. To address these 082 challenges, we propose a unified MLLM-based layout model that generates layouts in natural 083 language formats, simultaneously optimizing composite and individual elements, ensuring geometric 084 plausibility and visual harmony.

085 In summary, our main contributions are as follows.

- 086 (i) We introduce **AnyLayout-120K**, a large-scale instruction-driven layout dataset that features four 087 sub-tasks composed of user instructions and interleaved multimodal design elements. Alongside 088 this dataset, we propose 7 geometry-aware metrics to ensure a more comprehensive assessment.
- 089 (ii) In addition to providing placements for individual design elements, we propose composite lay- 090 outs that describe the overall design layout. These composite layouts can be seamlessly integrated 091 into T2I models, facilitating the effective rendering of the generated designs.
- 092 (iii) We establish a strong baseline that achieves state-of-the-art performance across tasks, providing 093 a foundation for future research in instruction-driven layout design.

## 095 2 RELATED WORK

097 **Content-Agnostic Layout Generation.** Early work abstracts layouts into elements with categorical 098 labels and geometric parameters, focusing on structural and spatial alignment while ignoring semantic 099 context. Representative models include GAN-based LayoutGAN (Li et al., 2019), VAE-based 100 LayoutVAE (Jyothi et al., 2019), and Transformer-VAE hybrids such as VTN (Arroyo et al., 2021) 101 and bidirectional masked BLT (Kong et al., 2022), which balance global alignment with diversity. 102 Beyond diffusion models, Flow Matching approaches like LayoutFlow (Guerreiro et al., 2024) and 103 discrete diffusion with external correction as in Layout-Corrector (Iwai et al., 2024) improve conver- 104 gence stability and geometric controllability. While these paradigms provide strong structural priors, 105 they lack multimodal semantic adaptation needed in real-world advertising and poster design.

106 **Content-Aware Visual-Textual Layout.** Content-aware methods tailor layouts to specific inputs 107 such as products, slogans, and backgrounds. CGL-GAN (Zhou et al., 2022) generates design lay- 108 outs from image composition and introduces metrics aligned with aesthetic intuition. PosterLay-

108 out (Hsu et al., 2023) models non-empty canvases and design order, establishing benchmarks and  
 109 evaluation criteria. AutoPoster (Lin et al., 2023) explores human–AI co-creation workflows for  
 110 advertising posters. LayoutFormer++ (Jiang et al., 2023) unifies multiple conditional tasks via  
 111 constraint serialization, while DETR-based LayoutDETR (Yu et al., 2024) demonstrates the strength  
 112 of detection-style representations for multimodal conditional layouts. Although these works have  
 113 enriched datasets and metrics, most assume fixed or partially pre-filled canvases, limiting general-  
 114 ization to common scenarios like “pure slogan”, “single product”, or “background-only” inputs.

115 **Layout Generation with MLLMs.** Recent work leverages LLMs and MLLMs to convert layouts  
 116 into structured, executable formats (e.g., HTML/JSON), enhancing interpretability and consistency.  
 117 LayoutNUWA (Tang et al., 2023) pioneered “code-based” layouts with improved semantic align-  
 118 ment via instruction tuning. PosterLlama (Seol et al., 2024) and PosterLLaVA (Yang et al., 2024)  
 119 adapt layout generation into LLM/MLLM pipelines, enabling natural language constraints, editable  
 120 SVGs, and multimodal interaction. VASCAR (Zhang et al., 2024) iteratively refines layouts through  
 121 visual self-correction in LVLMs. Strong multimodal base models such as Qwen2.5-VL (Bai et al.,  
 122 2025)—with fine-grained localization and document/graph parsing capabilities—form the infras-  
 123 tructure for end-to-end instruction-to-layout training and evaluation. Aligned with our work, these  
 124 approaches advocate a *unified task interface* plus *executable structural outputs*, paving the way for  
 125 cross-task alignment and downstream renderability.

### 126 3 ANYLAYOUT DATASET

127 We extend layout generation from fixed-canvas settings to a *versatile, instruction-driven* formu-  
 128 lation that supports multimodal inputs (*slogan-only, textual product, visual product, visual back-*  
 129 *ground*). Specifically, we contribute: (i) a unified task interface covering the four sub-tasks  
 130 (Fig. 1), (ii) AnyLayout-120K, a large-scale instruction-driven dataset and (iii) geometry-aware,  
 131 task-conditioned metrics that enhance the prior assessments used in CGL/PKU. This section is orga-  
 132 nized as follows: Sec. 3.1 introduces the four sub-tasks; Sec. 3.2 presents product-centered metrics  
 133 and Sec. 3.3 outlines a four-stage data construction pipeline.

#### 134 3.1 PROPOSED TASK

135 Given an optional pair of images (product/background) and the instructions input, the task is re-  
 136 quired to output not only the placement of individual design elements, but also the composite layout  
 137 to support downstream T2I model to generate poster. We therefore cast layout generation as an  
 138 instruction-driven design problem, closer to real practice than fixed-canvas formulations. As illus-  
 139 trated in Fig. 1, we define four sub-tasks: (1) ***Slogan Layout***, (2) ***Textual Product Layout***, (3) ***Visual***  
 140 ***Product Layout***, and (4) ***Visual Background Layout***.

141 ***Slogan Layout.*** This task aims to generate optimal poster layouts from textual slogans, particularly  
 142 for cases containing only text, such as exhibition themes or cultural promotion posters. The task  
 143 requires the text’s position, scale, and arrangement solely based on the given slogan.

144 ***Textual Product Layout.*** This task addresses practical poster-generation needs where layouts are  
 145 derived solely from textual descriptions of a product, complemented by slogans or other elements.  
 146 For example, it may involve creating a face cream-selling poster featuring a green-scene background  
 147 and a specific slogan. Effective design in such cases requires accurately interpreting the concepts in  
 148 the text and arranging the elements with precise spatial organization.

149 ***Visual Product Layout.*** Building on the product-description task, a more constrained and practical  
 150 scenario incorporates the product image alongside the text slogan as input. The task requires a  
 151 poster layout that seamlessly integrates visual and textual elements, aligning layout geometry with  
 152 semantic content. This necessitate reasoning about relative positioning, scale, and visual hierarchy  
 153 under the constraints of real image inputs.

154 ***Visual Background Layout.*** A common application scenario involves incorporating a text slogan  
 155 layout frame into a poster image that already contains a primary product and background. In our  
 156 proposed task, the input consists solely of the slogan, without specifying the dimensions of the text  
 157 layout or providing category and size information for any additional layout elements to be predicted.

Dataset	Instr. Driven	Input Design Elements	Output	Slogan Lang.	Aspect Ratio
CGL	✗	Back.Img(Op) & Cate/Size	Layout	CN	(2:3)
AP	✗	Back.Img(Op) & Cate/Size	Layout	CN	(2:3)
PKU	✗	Back.Img(Op) & Cate/Size	Layout	CN	(2:3)
<b>AnyLayout-120K</b>	✓	Back/Prod.Img(Op) & Instruction	Layout & Composite	CN, EN	(2:3),(1:1)

Table 1: Comparison of AnyLayout-120K with existing poster layout datasets. *Instr. Driven* denotes support for explicit, user instruction–driven generation. *Input Design Elements* describes the optional or required inputs: *Back.Img* means a poster background with product already placed, *Op* = optional, *Cate/Size* = assigned category or bounding-box size, *Back/Prod.Img(Op)* = poster background or product image provided optionally, plus instructions, categories, and slogans. *Output* lists what the model generates: conventional layouts or extended composite layouts combining semantic and geometric information. *Slogan Lang.* shows supported languages for slogans. *Aspect Ratio* lists available layout aspect ratios.

### 3.2 PRODUCT-CENTERED METRICS

We introduce new evaluation metrics from a product-centered perspective, as existing content-layout benchmarks do not involve product placement and interaction. Drawing inspiration from typographic and layout studies (Ma et al., 2024; Rebelo et al., 2024) as well as established graphic design principles (Ngo et al., 2000; Harrington et al., 2004), we propose task-conditioned, geometry-aware metrics. These metrics aim to provide a more comprehensive assessment of layout designs, specifically focusing on the effective integration of products within the overall composition.

Each metric is a *geometry functional* that operates solely on predicted and ground-truth box coordinates. The metrics include: Centrality Score (*CS*), Size Ratio Norm (*SR<sub>Norm</sub>*), Overlap Score (*OS*), Vertical Position Score (*VPS*), Pair Distance Score (*PDS*), Dispersion Consistency Score (*DCS*), and Size Consistency Score (*SCS*). Together, these metrics effectively capture both aesthetic alignment (e.g., balance and hierarchy) and functional positioning (e.g., occlusion avoidance and scale consistency).

The *CS* measures how close the product’s center is to the poster’s center, with higher scores awarded for more central placements:

$$CS = 1 - \frac{d}{d_{max}}$$

$$d_{max} = \sqrt{(W/2)^2 + (H/2)^2}$$

$$d = \sqrt{(c_x - W/2)^2 + (c_y - H/2)^2} \quad (1)$$

where  $(c_x, c_y)$  is the product-box center. If  $d=0$ , then  $CS=1$ ; if  $d=d_{max}$ , then  $CS=0$ .

The *SR<sub>Norm</sub>* encourages a product area within a desirable range; overly small boxes are penalized linearly, while overly large boxes are saturated at the upper bound:

$$SR_{Norm} = \frac{\min(\frac{A_{prod}}{A_{img}}, S_{max})}{S_{max}} \quad (2)$$

$$A_{prod} = (x_2 - x_1)(y_2 - y_1)$$

$$A_{img} = W \times H$$

here  $(x_1, y_1)$  and  $(x_2, y_2)$  are the top-left and bottom-right corners of the product box, and  $S_{max}$  is the upper-area threshold.

The *OS* penalizes occlusion between the product and other elements (text, underlay, etc.):

$$OS = 1 - \frac{\sum_i \text{Area of Intersection}(prod, other_i)}{A_{prod}} \quad (3)$$

The *VPS* encourages the product to sit near a task-specific vertical target (e.g., lower-center emphasis);  $t \in [0, 1]$  controls the preferred normalized vertical position:

$$VPS = 1 - \frac{\frac{c_y}{H} - t}{\max(t, 1 - t)} \quad (4)$$

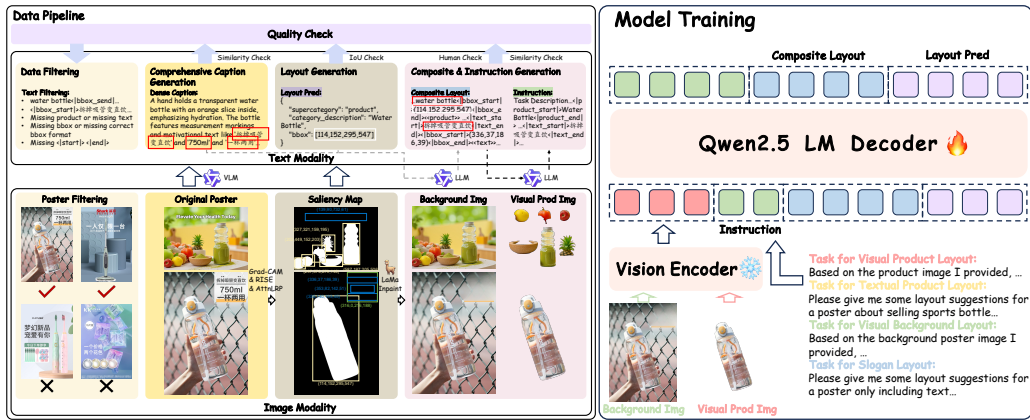


Figure 2: Our data processing pipeline for image and text modality inputs, along with the model training framework.

For multi-product cases, promotes reasonable spacing by averaging pairwise center distances— $PDS$  (normalized by the image diagonal):

$$PDS = \frac{1}{N} \sum_{i < j} \frac{d_{ij}}{\sqrt{W^2 + H^2}} \quad (5)$$

where  $d_{ij}$  is the Euclidean distance between centers of boxes  $i$  and  $j$ , and the sum runs over all unordered pairs (the  $1/N$  factor denotes averaging).

The  $DCS$  measures the uniformity of inter-product spacing via the coefficient of variation:

$$DCS = 1 - \mathcal{CV}(\{\frac{d_{ij}}{\sqrt{W^2 + H^2}}\}), \quad (6)$$

where  $\mathcal{CV} = \sigma/\mu$  is the coefficient of variation. More uniform distances (smaller  $\mathcal{CV}$ ) yield higher scores.

The  $SCS$  encourages comparable product scales by penalizing variation in area ratios:

$$SCS = 1 - \mathcal{CV}(\{\frac{A_i}{WH}\}_{i=1}^N) \quad (7)$$

### 3.3 DATA PIPELINE

To support the four instruction-driven tasks in Sec. 3.1, we build a systematic, mutually validating dataset pipeline (Fig. 2) with **five** stages: **(1) Data Filtering**, **(2) Comprehensive Caption Generation**, **(3) Layout Generation**, **(4) Composite & Instruction Generation**, and **(5) Quality Check**. This structure mirrors our product-centered metrics in Sec. 3.2, ensuring that data construction, validation, and evaluation use consistent geometry-aware criteria.

To this end, we address the scarcity of *instruction-driven* resources for controllable poster layout by converting four heterogeneous datasets—PKU (Hsu et al., 2023), AutoPoster (AP) (Lin et al., 2023), CGL (Li et al., 2023), and CreatiDesign (CD) (Zhang et al., 2025a)—into a unified dataset tailored for multimodal *instruction-driven* fine-tuning. Beyond raw coordinates, each sample is augmented with a complete *instruction-driven* pair: natural-language task description, multimodal context, and a machine-verifiable structured answer.

**Data Filtering.** To remove annotation noise in multi-product posters from PKU/AP/CGL, we retained 60K single-product samples via Data Filtering. For the multi-product, 60K samples were randomly selected from CD. These two subsets were then combined to form the original 120K-poster layout dataset. Furthermore, Data Filtering employs a simultaneous filtration process on the data subsequent to Quality Check, ensuring the establishment of a high-quality dataset.

**Comprehensive Caption Generation & Layout Generation.** Following GoT (Fang et al., 2025), we pair boxes with descriptive captions encoding spatial and semantic layout information. We implement captioning with Qwen2.5-VL (Bai et al., 2025) using a prompt that covers: (1) fine-grained

270 product description, (2) background composition/style, (3) typography/decorations, and (4) slogan  
 271 content/placement. To correct occasional slogan errors, we align generated captions to ground-truth  
 272 slogans via semantic similarity matching, repair mismatches, and filter low-alignment cases (Fig. 2).  
 273

274 For Layout Generation, text/background boxes are taken from original labels. For visual-product  
 275 localization, we compute *model-agnostic* saliency and convert it to boxes via morphology and  
 276 connected components: apply Grad-CAM (Selvaraju et al., 2017) on a product-recognition encoder  
 277 and cross-validate with RISE (Petsiuk et al., 2018) to reduce model-specific bias; threshold the  
 278 consensus map, extract the maximal connected component, and fit a tight box. Low-confidence  
 279 or multi-peak cases fall back to attention-rollout via AttnLRP (Chefer et al., 2021) to preserve re-  
 280 call. We binarize with Otsu+area priors, generate candidates, and select the top-confidence box with  
 281 non-maximum suppression. This yields accurate product localization (Fig. 2), and—together with  
 282 refined captions—forms a compact, executable multimodal annotation.

283 **Composite & Instruction Generation.** After captioning and layout generation, we refine  
 284 captions with Qwen3 (Yang et al., 2025) to inject explicit layout references then gain the  
 285 Layout-Aware Composite. The module aligns caption spans to regions by semantic simi-  
 286 larity and replaces matched phrases with structured placeholders  $<|box\_start|>\dots<|box\_end|>\langle\langle$ product/logo/text/underlay/embellishment $\rangle\rangle$  (Fig. 2), enabling pre-  
 287 cise text–geometry linkage.

288 For instruction generation, we collected high-quality user input based on actual design requirements  
 289 and had Qwen3 refine it based on the composite. This refinement retained the necessary visual prod-  
 290 uct and slogan layout elements, as well as the poster aspect ratio, within the instructions. The layout  
 291 elements were then matched with the special symbols  $<|product\_start|>\dots<|product\_end|>$  and  
 292  $<|text\_start|>\dots<|text\_end|>$ , respectively, to complete the different instruction set for  
 293 four task scenarios (see the Appendix for more instruction set examples).

294 Both Composite generation and Instructions generation will undergo similarity check for the vi-  
 295 sual product and slogan first. Then we quantify quality via human check under a stratified proto-  
 296 col. We sample  $n=400$  items from AnyLayout-120K, stratified by the four tasks ( $4 \times 100$ ) and by  
 297 single/multi-product (50/50). The reviewer judges (i) *box correctness* (product/text/underlay accept-  
 298 able if IoU to intended region  $\geq 0.7$  or justified tightness) and (ii) *caption–box alignment*.

299 **Quality Check.** To estimate datasets quality including VLM/LLM generation results and visual  
 300 product layout generation results, we deploy a deterministic validator consisting of *Similarity Check*,  
 301 *IoU Check* and *Human Check*:

- 302 • *Similarity Check*: we apply it on *Comprehensive Caption Generation* and *Composite &*  
 303 *Instruction Generation*. It is used to check the VLM/LLM generated slogan and the visual  
 304 product whether match the ground-truth.
- 306 • *IoU Check*: we mainly utilize it on *Layout Generation*. Then, we check the visual product  
 307 location quality by requiring IoU ( $>0.6$ ) agreement between Grad-CAM and RISE other-  
 308 wise fall back to attention-rollout AttnLRP.
- 309 • *Human Check*: we let human reviewer to check a gold sample of Composite and Instruction  
 310 generated by LLM whether the layout element match the correct slogan or visual product.

312 Across Quality Check, the *Similarity Check* and *IoU check* accepts 92.5% ( $\pm 2.1\%$ ) of samples;  
 313 among these, the *Human Check* confirms 95.1% ( $\pm 1.9\%$ ) box correctness and 96.4% ( $\pm 2.0\%$ )  
 314 caption–box alignment. Combining (i) *Similarity & IoU* pass and (ii) *Human Check* pass yields an  
 315 end-to-end clean-label estimate of 93.7% ( $\pm 2.9\%$ ).

## 317 4 METHOD

### 318 4.1 UNIFIED LAYOUT MODEL

321 Recent MLLM studies report emergent layout understanding and the ability to interpret spatial co-  
 322 ordinates for coherent layout generation (Seol et al., 2024; Zhang et al., 2024; Chen et al., 2025a;  
 323 Tang et al., 2023). To validate our task design and the utility of AnyLayout-120K, we build an SFT  
 baseline on Qwen2.5VL-7B.

324 **Single-task SFT.** We first fine-tune four *single-task* models. Each output is a JSON-like sequence  
 325 containing *category*, *short description*, and *bbox* for every element. Training minimizes the next-  
 326 token cross-entropy:

$$327 \quad 328 \quad 329 \quad \mathcal{L}_{CE} = - \sum_{i=1}^N y_i \log(p_i) \quad (8)$$

330 computed over the serialized instruction–response.

331 **Unified multi-task SFT.** We then train a *single* model across all four tasks using a balanced  
 332 1:1:1:1 sampler with randomized batch shuffling. This exposes the model to heterogeneous in-  
 333 put regimes (*slogan-only*, *textual/visual product*, *visual background*) and encourages transfer of  
 334 geometry–semantics priors across tasks. In practice, joint training yields consistently better average  
 335 performance than isolated training, indicating useful cross-task synergies.

## 337 4.2 COMPOSITE LAYOUT PREDICTION

338 Layout prediction requires reasoning over *what* (semantics) and *where/how* (geometry, scale, hierar-  
 339 chy) jointly. Rather than designing task-specific heads, we serialize an *executable composite layout*  
 340 that captures element types, semantic attributes, and inter-element geometric relations in a single  
 341 sequence. This reframes the problem from independent coordinate regression to autoregressive *joint*  
 342 *geometry–semantics* reasoning. For example, two elements—a visual product “*face cream*” and a  
 343 slogan “*Double points for luxury formal wear*”—are emitted as a compact description with their  
 344 *bboxes* embedded at the points where they are referenced.

345 Compared with composite-oriented frameworks such as PosterLlama (Seol et al., 2024), Poster-  
 346 LLaVA (Yang et al., 2024), and LayoutNUWA (Tang et al., 2023), our formulation differs in two  
 347 geometric aspects: (i) we *merge* textual semantics and coordinates into one executable sequence that  
 348 encodes cross-element constraints, enabling stepwise reasoning in a single state space; (ii) the same  
 349 composite space is *instruction-compatible* across all input modalities (*slogan-only*, *textual/visual*  
 350 *product*, *visual background*), avoiding fixed-canvas or placeholder-only assumptions and eliminat-  
 351 ing task-specific decoders.

352 All four subtasks are projected into this common composite space, allowing the unified model to  
 353 learn transferable design priors. The representation serves as a *binding contract* to downstream  
 354 renderers: predicted sequences can be directly executed to produce layouts. While our baseline  
 355 uses Qwen2.5-VL-7B with instruction tuning, the formulation is model-agnostic and invites future  
 356 architectures tailored for composite layout reasoning.

## 357 5 EXPERIMENT

### 359 5.1 EXPERIMENT SETTINGS

361 **Datasets.** We evaluate on **AnyLayout**, comprising five element types—logo, text, product, un-  
 362 derlay, and embellishment. The dataset contains 126,131 annotated *poster–layout* pairs, split into  
 363 118,450 for training and 7,681 for testing. Following our data pipeline, AnyLayout aggregates four  
 364 sources: CGL (train 20,851 / test 1,026), AutoPoster (train 31,495 / test 3,655), PKU (train 6,726),  
 365 and CreatiDesign (train 59,378 / test 3,000). Training data covers four novel tasks with product/-  
 366 text annotations (including product and background images), while the test set contains annotated  
 367 samples for each task.

368 **Evaluation Metrics.** We adopt: (1) PKU (Hsu et al., 2023) and CGL (Li et al., 2023) content-  
 369 aware layout benchmarks; (2) a new single-/multi-product benchmark. PKU metrics include *ali*,  
 370 *und<sub>l</sub>*, *und<sub>s</sub>*, *ove*, and *val*; CGL metrics comprise *R<sub>ove</sub>*, *R<sub>und</sub>*, *R<sub>ali</sub>*, and *R<sub>occ</sub>*. *R<sub>occ</sub>* / *val* measure  
 371 unused or invalid layout space, *R<sub>ali</sub>* / *ali* assess element alignment, *ove* / *R<sub>ove</sub>* (via IoU) quantify  
 372 non-decorative element overlap, and *R<sub>und</sub>* / *und<sub>l</sub>* / *und<sub>s</sub>* evaluate the enhancement from decorative  
 373 to non-decorative elements.

374 **Baseline.** Our goal is to validate the *AnyLayout* task, dataset, and unified benchmarks. We  
 375 benchmark mainstream multimodal layout predictors—PosterLlama (Seol et al., 2024), Poster-  
 376 LLaVA (Yang et al., 2024)—in zero-shot mode (due to mismatched I/O formats) and compare with  
 377 Qwen2.5VL-7B (Bai et al., 2025) zero-shot outputs, serving as a baseline for our SFT and *SFT w/ C* approaches.

Tasks		PKU Metrics						CGL Metrics				
Methods	Tasks	<i>ali</i> ↓	<i>und<sub>l</sub></i> ↑	<i>und<sub>s</sub></i> ↑	<i>ove</i> ↓	<i>val</i> ↑	<i>R<sub>ove</sub></i> ↓	<i>R<sub>und</sub></i> ↑	<i>R<sub>ali</sub></i> ↓	<i>R<sub>occ</sub></i> ↑		
Zero-shot	Slogan Layout	0.0236	0.8451	0.3485	0.2778	<b>1.0</b>	0.4637	0.8523	0.0264	0.7139		
SFT w/ C	Slogan Layout	0.0241	0.9863	0.9775	0.0038	0.9998	0.0093	0.9896	0.0148	<b>0.9644</b>		
SFT w/ C	Mix	0.0208	<b>0.9951</b>	<b>0.9900</b>	<b>0.0021</b>	0.9998	0.0050	<b>0.9965</b>	0.0098	<b>0.9644</b>		
SFT		<b>0.0160</b>	0.9901	0.9875	0.0023	0.9997	<b>0.0042</b>	0.9922	<b>0.0030</b>	0.9621		
PosterLlama		0.0229	0.8681	0.5550	0.2677	0.9995	0.4526	0.8613	0.0252	0.8250		
PosterLLaVA		0.0214	0.8857	0.5679	0.2523	0.9996	0.4482	0.8766	0.0241	0.8357		
Zero-shot	Txt Prod Layout	0.0225	0.9334	0.9301	0.0222	<b>1.0</b>	0.0486	0.9336	0.0046	0.8848		
SFT w/ C	Txt Prod Layout	<b>0.0168</b>	0.9818	0.9688	0.0123	0.9998	0.0277	0.9813	0.0050	<b>0.9869</b>		
SFT w/ C	Mix	0.0229	<b>0.9829</b>	<b>0.9787</b>	<b>0.0021</b>	0.9999	<b>0.0043</b>	0.9844	<b>0.0039</b>	0.9836		
SFT		0.0195	0.9803	0.9767	0.0032	0.9997	0.0056	<b>0.9928</b>	0.0040	0.9712		
PosterLlama		0.0218	0.9002	0.8915	0.0206	0.9996	0.0469	0.8987	0.0063	0.8991		
PosterLLaVA		0.0210	0.9018	0.8874	0.0194	0.9999	0.0435	0.9011	0.0051	0.9008		
Zero-shot	Vis Prod Layout	0.1000	0.7860	0.6407	0.2759	<b>1.0</b>	0.3797	0.7912	0.0325	0.8410		
SFT w/ C	Vis Prod Layout	0.0243	0.9777	0.9701	0.0104	0.9999	0.0149	0.9777	0.0070	0.9817		
SFT w/ C	Mix	0.0224	<b>0.9916</b>	<b>0.9886</b>	<b>0.0024</b>	0.9999	<b>0.0052</b>	<b>0.9917</b>	<b>0.0062</b>	<b>0.9823</b>		
SFT		<b>0.0193</b>	0.9877	0.9852	0.0032	0.9997	0.0054	0.9915	0.0069	0.9689		
PosterLlama		0.0872	0.8016	0.6527	0.2431	0.9995	0.3369	0.8054	0.0258	0.8722		
PosterLLaVA		0.0695	0.8136	0.6473	0.2289	0.9996	0.3077	0.8152	0.0258	0.8814		
Zero-shot	Vis Bg Layout	0.0463	0.6442	0.4758	0.2262	<b>1.0</b>	0.3657	0.6462	0.0172	0.8686		
SFT w/ C	Vis Bg Layout	<b>0.0126</b>	0.9689	0.9612	0.0140	0.9996	0.0206	0.9739	0.0058	<b>0.9802</b>		
SFT w/ C	Mix	0.0134	<b>0.9908</b>	<b>0.9848</b>	<b>0.0039</b>	0.9997	<b>0.0069</b>	<b>0.9905</b>	<b>0.0038</b>	<b>0.9802</b>		
SFT		0.0131	0.9871	0.9794	0.0060	0.9991	0.0091	0.9890	0.0039	0.9745		
PosterLlama		0.0461	0.6970	0.5489	0.2127	0.9995	0.3599	0.6976	0.0166	0.8710		
PosterLLaVA		0.0432	0.7315	0.5264	0.2038	0.9995	0.3571	0.7296	0.0170	0.8826		

Table 2: Experiment results on AnyLayout-test (w/o product). *Txt*, *Prod*, *Vis*, *Bg* denote *Textual*, *Product*, *Visual*, and *Background*. Best performance per column is in **bold**.

Tasks		Single Product Metrics ↑						Multi Product Metrics ↑					
Methods	Tasks	<i>CS</i>	<i>SR<sub>Norm</sub></i>	<i>OS</i>	<i>VPS</i>	<i>MeanIoU</i>	<i>CPS</i>	<i>CPS</i>	<i>MeanIoU</i>	<i>PDS</i>	<i>DCS</i>	<i>SCS</i>	<i>CPS<sub>m</sub></i>
Zero-shot	Vis Prod Layout	0.7488	<b>0.9987</b>	0.6482	0.7830	0.4233	0.7946	0.6182	0.2219	0.1957	<b>0.7821</b>	0.3894	0.4964
SFT w/ C	Vis Prod Layout	0.7847	0.9605	0.9357	0.8876	<b>0.7512</b>	0.8921	0.6819	<b>0.4332</b>	<b>0.2479</b>	0.7040	0.3820	<b>0.5040</b>
SFT w/ C	Mix	<b>0.7850</b>	0.9656	<b>0.9424</b>	0.8880	0.7061	<b>0.8952</b>	<b>0.6876</b>	0.3923	0.2375	0.7007	0.3760	0.5005
SFT		0.7835	0.9644	0.9378	<b>0.8947</b>	0.7274	0.8950	0.6502	0.3030	0.2258	0.7156	<b>0.4087</b>	0.5001
PosterLlama		0.7415	0.9940	0.6702	0.7917	0.4259	0.7993	0.6257	0.2306	0.1981	0.7124	0.3925	0.4822
PosterLLaVA		0.7541	0.9948	0.6539	0.8002	0.4310	0.8008	0.6284	0.2517	0.2005	0.7294	0.3901	0.4871
Zero-shot	Txt Prod Layout	0.8882	<b>1.0</b>	0.7737	0.7940	0.4689	0.8640	0.6074	0.1445	0.2593	0.6054	0.4417	0.4785
SFT w/ C	Txt Prod Layout	0.7874	0.9543	0.9304	0.8868	<b>0.6264</b>	0.8897	0.6348	0.1985	0.2542	0.6864	0.4395	0.5038
SFT w/ C	Mix	0.7941	0.9623	0.9293	<b>0.8952</b>	0.5959	<b>0.8953</b>	<b>0.6934</b>	<b>0.2643</b>	0.2465	<b>0.6927</b>	0.3911	<b>0.5059</b>
SFT		0.7901	0.9639	<b>0.9332</b>	0.8903	0.6060	0.8943	0.6501	0.2074	0.2247	0.6917	0.4312	0.4994
PosterLlama		0.8820	0.9983	0.7479	0.7825	0.4438	0.8527	0.6095	0.1507	0.2588	0.6106	0.4439	0.4807
PosterLLaVA		<b>0.8952</b>	0.9847	0.7563	0.7801	0.4695	0.8541	0.6194	0.1689	<b>0.2653</b>	0.6055	<b>0.4510</b>	0.4853

Table 3: Comparison of **Single Product** and **Multi Product** metrics for different methods. *Txt*, *Prod*, *Vis* denote *Textual*, *Product*, and *Visual* respectively. Best performance per column is in **bold**.

**Implementation Details.** Based on Qwen-2.5-VL-7B (Bai et al., 2025), we fine-tune our model with the following experiment settings: learning rate of 1.0e-5, global batch size of 16, and image maximum input resolution is set to 1024 × 1024 pixels. We utilize LLaMA-Factory (Zheng et al., 2024) as our supervised fine-tuning (SFT) codebase. We perform SFT on our proposed AnyLayout-120K dataset for 3 epochs with 8 NVIDIA H20 GPUs, and the training steps are the same for the model trained with extra reasoning process.

## 5.2 MAIN RESULTS

Tab. 2 reports PKU/CGL results for the four sub-tasks; Tab. 3 gives our single-/multi-product metrics assessing spatial alignment, scale consistency, and inter-object arrangement. Fig. 3 visualizes the full pipeline: AnyLayout predicts category, bounding box, localized text, product description, and a composite layout string; the latter conditions Flux-Kontext (Labs et al., 2025) to render layouts faithful to semantics and spatial constraints.

Relative to zero-shot Qwen2.5VL, all SFT variants achieve substantial gains across PKU (*ali* ↓, *und* ↑, *ove* ↓, *val* ↑) and CGL (*R<sub>ove</sub>* ↓, *R<sub>und</sub>* ↑, *R<sub>ali</sub>* ↓, *R<sub>occ</sub>* ↑) for every task. Improvements carry over to product-centric metrics (Tab. 3), where SFT consistently boosts *CS*, *OS*, *VPS*, *MeanIoU*, *CPS*, and their multi-product counterparts.

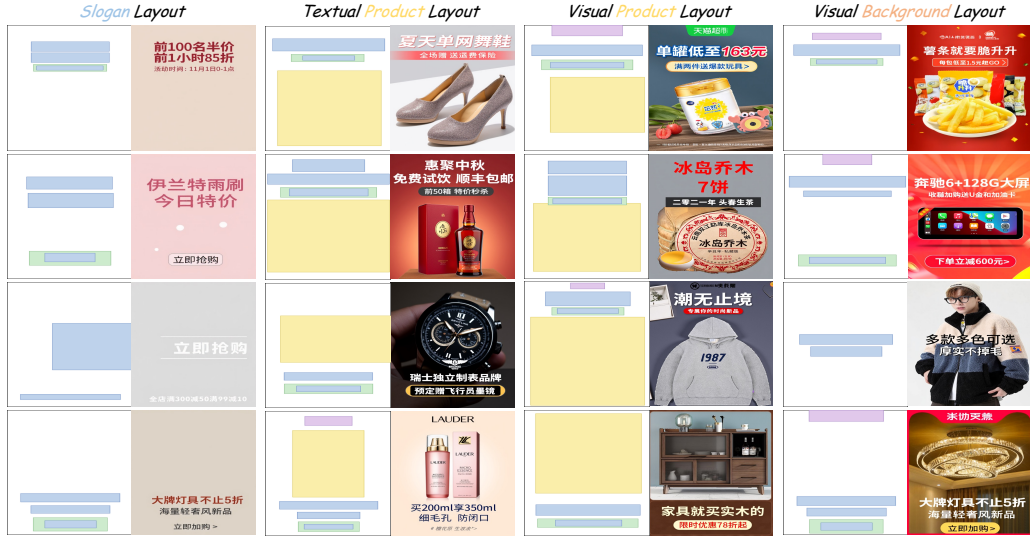


Figure 3: Qualitative results on AnyLayout test set, each sub-task is displayed in a separate column.

Across both PKU and CGL, PosterLlama and PosterLLaVA lag behind any SFT-trained AnyLayout; PosterLLaVA generally outperforms PosterLlama (e.g., better *und* and lower  $R_{ove}$ ), with rare reversals. Under our proposed metrics, the same pattern holds—PosterLLaVA slightly leads in *VPS/MeanIoU/CPS* for *Vis Prod Layout*—yet both are far below SFT models.

System-level ranking is consistent across benchmarks: *SFT w/ C*  $\approx$  *SFT* > zero-shot Qwen2.5VL  $>$  PosterLLaVA  $>$  PosterLlama, with minor variations on columns like *OS* or *SCS*. This stability across legacy and proposed metrics indicates the latter capture capability gaps aligned with established criteria while being more sensitive to product placement and compositional fidelity.

### 5.3 ABLATION STUDIES

**Mix Training.** Multi-task training (*SFT w/ C*, *Mix*) surpasses single-task SFT on most metrics, particularly improving spatial/scale consistency (*VPS*, *MeanIoU*, *CPS*, *CPS<sub>m</sub>*) without degrading category or overlap scores, confirming that shared task structure promotes generalization.

**Composite Layout.** Compared to plain SFT, *SFT w/ C* yields consistent PKU gains and dominates on CGL for *Vis Prod Layout* and *Vis Bg Layout*, with improvements in most metrics for *Txt Prod Layout* and *Slogan Layout*. Similar trends appear in Table 3, where composite layouts improve most single-/multi-product metrics. This suggests composite layout strings provide a strong inductive bias for coherent interactions among text, product, and background—advantages retained when rendered with Flux-Kontext (Labs et al., 2025).

## 6 CONCLUSION

In this paper, we propose **AnyLayout-120K**, a comprehensive dataset and benchmark for advertising poster layout generation, which advances the field through four diverse sub-tasks, rich design varieties, and language-conditioned layout prediction. Based on the proposed dataset, we present an MLLM-based model as a strong baseline, which unifies composite and fine-grained spatial reasoning through natural languages with product or background images as optional visual inputs, enabling coherent and context-aware layout generation. Extensive experiments demonstrate consistent superiority over existing methods on different tasks and metrics. In short, AnyLayout establishes a new paradigm for layout modeling by integrating semantic understanding, structural control, and cross-modal generation with one single model, representing a significant step toward scalable, intelligent design automation in complex, real-world scenarios.

486 7 REPRODUCIBILITY STATEMENT  
487

488 To ensure the full reproducibility of our findings, we have provided comprehensive implementation  
489 details throughout the paper. Each four tasks I/O examples to describe our datasets at Sec. 3 and  
490 Appendix A.1. Key details of instructions we reformulates them based on four tasks are presented  
491 on Sec. 3.3 and Appendix A.2. Moreover, AnyLayout-120K datasets analysis is discussed at Ap-  
492 pendix A.3 and baseline architecture of AnyLayout framework is described at Sec. 4. In line with  
493 our commitment to open science, AnyLayout-120K dataset and source code will be made publicly  
494 available.

495 8 ETHICS STATEMENT  
496

497 This research adheres to the ICLR Code of Ethics in all aspects of its execution, including data  
498 collection, analysis, and dissemination of results. The study does not involve human subjects, animal  
499 experiments, or sensitive personal data. All datasets used are publicly available and were collected  
500 in compliance with applicable laws and licenses. We have reviewed the datasets to the best of our  
501 ability to minimize potential bias, discrimination, or unfairness, and to avoid inclusion of harmful  
502 or offensive content.

503 The methods proposed pose no foreseeable risk to individuals, groups, or the environment, and are  
504 intended for academic and socially beneficial purposes. Any potential misuse scenarios have been  
505 considered and mitigated through appropriate design choices. No conflicts of interest or sponsor-  
506 ships that could have influenced the results are present. All results are reported honestly, without  
507 fabrication, falsification, or inappropriate manipulation, in line with the principles of research in-  
508 tegrity.

509 By including this statement, the authors explicitly acknowledge their obligation to comply with the  
510 ICLR Code of Ethics throughout the submission, review, and discussion process.

512 REFERENCES  
513

514 Diego Martin Arroyo, Janis Postels, and Federico Tombari. Variational transformer networks for  
515 layout generation. In *Proceedings of the IEEE/CVF Conference on Computer Vision and Pattern*  
516 *Recognition*, pp. 13642–13652, 2021. 2

518 Shuai Bai, Keqin Chen, Xuejing Liu, Jialin Wang, Wenbin Ge, Sibo Song, Kai Dang, Peng Wang,  
519 Shijie Wang, Jun Tang, et al. Qwen2. 5-vl technical report. *arXiv preprint arXiv:2502.13923*,  
520 2025. 3, 5, 7, 8

521 Souradeep Chakraborty, Zijun Wei, Conor Kelton, Seoyoung Ahn, Aruna Balasubramanian, Gre-  
522 gory J Zelinsky, and Dimitris Samaras. Predicting visual attention in graphic design documents.  
523 *IEEE Transactions on Multimedia*, 25:4478–4493, 2022. 2

525 Hila Chefer, Shir Gur, and Lior Wolf. Transformer interpretability beyond attention visualization.  
526 In *Proceedings of the IEEE/CVF conference on computer vision and pattern recognition*, pp.  
527 782–791, 2021. 6

528 Haoyu Chen, Xiaojie Xu, Wenbo Li, Jingjing Ren, Tian Ye, Songhua Liu, Ying-Cong Chen, Lei  
529 Zhu, and Xinchao Wang. Posta: A go-to framework for customized artistic poster generation.  
530 In *Proceedings of the Computer Vision and Pattern Recognition Conference*, pp. 28694–28704,  
531 2025a. 6

533 Rui Chen, Lei Sun, Jing Tang, Geng Li, and Xiangxiang Chu. Finger: Content aware fine-grained  
534 evaluation with reasoning for ai-generated videos. *arXiv preprint arXiv:2504.10358*, 2025b. 2

535 Yutao Cheng, Zhao Zhang, Maoke Yang, Hui Nie, Chunyuan Li, Xinglong Wu, and Jie Shao.  
536 Graphic design with large multimodal model. *arXiv preprint arXiv:2404.14368*, 2024. 2

538 Xiangxiang Chu, Limeng Qiao, Xinyu Zhang, Shuang Xu, Fei Wei, Yang Yang, Xiaofei Sun, Yiming  
539 Hu, Xinyang Lin, Bo Zhang, et al. Mobilevlm v2: Faster and stronger baseline for vision language  
model. *arXiv preprint arXiv:2402.03766*, 2024. 2

540 Rongyao Fang, Chengqi Duan, Kun Wang, Linjiang Huang, Hao Li, Shilin Yan, Hao Tian, Xingyu  
 541 Zeng, Rui Zhao, Jifeng Dai, et al. Got: Unleashing reasoning capability of multimodal large  
 542 language model for visual generation and editing. *arXiv preprint arXiv:2503.10639*, 2025. 5

543 Julian Jorge Andrade Guerreiro, Naoto Inoue, Kento Masui, Mayu Otani, and Hideki Nakayama.  
 544 Layoutflow: flow matching for layout generation. In *European Conference on Computer Vision*,  
 545 pp. 56–72. Springer, 2024. 2

546 Steven J Harrington, J Fernando Naveda, Rhys Price Jones, Paul Roetling, and Nishant Thakkar.  
 547 Aesthetic measures for automated document layout. In *Proceedings of the 2004 ACM symposium*  
 548 on Document engineering, pp. 109–111, 2004. 4

549 Hsiao Yuan Hsu, Xiangteng He, Yuxin Peng, Hao Kong, and Qing Zhang. Posterlayout: A new  
 550 benchmark and approach for content-aware visual-textual presentation layout. In *Proceedings of*  
 551 the IEEE/CVF Conference on Computer Vision and Pattern Recognition, pp. 6018–6026, 2023.  
 552 1, 3, 5, 7

553 HsiaoYuan Hsu and Yuxin Peng. Postero: Structuring layout trees to enable language models in  
 554 generalized content-aware layout generation. In *Proceedings of the Computer Vision and Pattern*  
 555 *Recognition Conference*, pp. 8117–8127, 2025. 2

556 Aaron Hurst, Adam Lerer, Adam P Goucher, Adam Perelman, Aditya Ramesh, Aidan Clark, AJ Os-  
 557 trow, Akila Welihinda, Alan Hayes, Alec Radford, et al. Gpt-4o system card. *arXiv preprint*  
 558 *arXiv:2410.21276*, 2024. 2

559 Shoma Iwai, Atsuki Osanai, Shunsuke Kitada, and Shinichiro Omachi. Layout-corrector: Alle-  
 560 viating layout sticking phenomenon in discrete diffusion model. In *European Conference on*  
 561 *Computer Vision*, pp. 92–110. Springer, 2024. 2

562 Zhaoyun Jiang, Jiaqi Guo, Shizhao Sun, Huayu Deng, Zhongkai Wu, Vuksan Mijovic, Zijiang James  
 563 Yang, Jian-Guang Lou, and Dongmei Zhang. Layoutformer++: Conditional graphic layout gen-  
 564 eration via constraint serialization and decoding space restriction. In *Proceedings of the IEEE/CVF*  
 565 *Conference on Computer Vision and Pattern Recognition*, pp. 18403–18412, 2023. 3

566 Akash Abdu Jyothi, Thibaut Durand, Jiawei He, Leonid Sigal, and Greg Mori. Layoutvae: Stochas-  
 567 tic scene layout generation from a label set. In *Proceedings of the IEEE/CVF International Con-*  
 568 *ference on Computer Vision*, pp. 9895–9904, 2019. 2

569 Xiang Kong, Lu Jiang, Huiwen Chang, Han Zhang, Yuan Hao, Haifeng Gong, and Irfan Essa. Blt:  
 570 Bidirectional layout transformer for controllable layout generation. In *European Conference on*  
 571 *Computer Vision*, pp. 474–490. Springer, 2022. 2

572 Black Forest Labs, Stephen Batifol, Andreas Blattmann, Frederic Boesel, Saksham Consul, Cyril  
 573 Diagne, Tim Dockhorn, Jack English, Zion English, Patrick Esser, et al. Flux. 1 kontext:  
 574 Flow matching for in-context image generation and editing in latent space. *arXiv preprint*  
 575 *arXiv:2506.15742*, 2025. 8, 9

576 Fengheng Li, An Liu, Wei Feng, Honghe Zhu, Yaoyu Li, Zheng Zhang, Jingjing Lv, Xin Zhu, Junjie  
 577 Shen, Zhangang Lin, et al. Relation-aware diffusion model for controllable poster layout genera-  
 578 tion. In *Proceedings of the 32nd ACM International Conference on Information and Knowledge*  
 579 *Management*, pp. 1249–1258, 2023. 5, 7

580 Jianan Li, Jimei Yang, Aaron Hertzmann, Jianming Zhang, and Tingfa Xu. Layoutgan: Gener-  
 581 ating graphic layouts with wireframe discriminators. In *International Conference on Learning*  
 582 *Representations*, 2019. 2

583 Jinpeng Lin, Min Zhou, Ye Ma, Yifan Gao, Chenxi Fei, Yangjian Chen, Zhang Yu, and Tiezheng  
 584 Ge. Autoposter: A highly automatic and content-aware design system for advertising poster  
 585 generation. In *Proceedings of the 31st ACM International Conference on Multimedia*, pp. 1250–  
 586 1260, 2023. 3, 5

587 Chunhao Lu, Qiang Lu, and Jake Luo. An explainable vision question answer model via diffusion  
 588 chain-of-thought. In *European Conference on Computer Vision*, pp. 146–162. Springer, 2024. 2

594 Yuhang Ma, Shanyuan Liu, Ao Ma, Xiaoyu Wu, Dawei Leng, and Yuhui Yin. Hico: Hierarchical  
 595 controllable diffusion model for layout-to-image generation. *Advances in Neural Information  
 596 Processing Systems*, 37:128886–128910, 2024. 4  
 597

598 Pablo Melendez and Clemens Havas. Spatial information integration in small language models for  
 599 document layout generation and classification. *arXiv preprint arXiv:2501.05497*, 2025. 2  
 600

601 David Chek Ling Ngo, Azman Samsudin, and Rosni Abdullah. Aesthetic measures for assessing  
 602 graphic screens. *J. Inf. Sci. Eng.*, 16(1):97–116, 2000. 4  
 603

604 Vitali Petsiuk, Abir Das, and Kate Saenko. Rise: Randomized input sampling for explanation of  
 605 black-box models. *arXiv preprint arXiv:1806.07421*, 2018. 6  
 606

607 Yifan Pu, Yiming Zhao, Zhicong Tang, Ruihong Yin, Haoxing Ye, Yuhui Yuan, Dong Chen, Jian-  
 608 min Bao, Sirui Zhang, Yanbin Wang, et al. Art: Anonymous region transformer for variable  
 609 multi-layer transparent image generation. In *Proceedings of the Computer Vision and Pattern  
 Recognition Conference*, pp. 7952–7962, 2025. 2  
 610

611 Yadong Qu, Shancheng Fang, Yuxin Wang, Xiaorui Wang, Zhineng Chen, Hongtao Xie, and Yong-  
 612 dong Zhang. Igd: Instructional graphic design with multimodal layer generation. *arXiv preprint  
 arXiv:2507.09910*, 2025. 2  
 613

614 Sérgio M Rebelo, Juan Julián Merelo, João Bicker, and Penousal Machado. Evaluation metrics  
 615 for automated typographic poster generation. In *International Conference on Computational  
 Intelligence in Music, Sound, Art and Design (Part of EvoStar)*, pp. 326–341. Springer, 2024. 4  
 616

617 Ramprasaath R Selvaraju, Michael Cogswell, Abhishek Das, Ramakrishna Vedantam, Devi Parikh,  
 618 and Dhruv Batra. Grad-cam: Visual explanations from deep networks via gradient-based local-  
 619 ization. In *Proceedings of the IEEE international conference on computer vision*, pp. 618–626,  
 620 2017. 6  
 621

622 Jaejung Seol, Seojun Kim, and Jaejun Yoo. Posterllama: Bridging design ability of language model  
 623 to content-aware layout generation. In *European Conference on Computer Vision*, pp. 451–468.  
 624 Springer, 2024. 3, 6, 7  
 625

626 Zecheng Tang, Chenfei Wu, Juntao Li, and Nan Duan. Layoutnuwa: Revealing the hidden layout  
 627 expertise of large language models. *arXiv preprint arXiv:2309.09506*, 2023. 3, 6, 7  
 628

629 An Yang, Anfeng Li, Baosong Yang, Beichen Zhang, Binyuan Hui, Bo Zheng, Bowen Yu,  
 630 Chang Gao, Chengen Huang, Chenxu Lv, et al. Qwen3 technical report. *arXiv preprint  
 arXiv:2505.09388*, 2025. 6  
 631

632 Tao Yang, Yingmin Luo, Zhongang Qi, Yang Wu, Ying Shan, and Chang Wen Chen. Posterllava:  
 633 Constructing a unified multi-modal layout generator with llm. *arXiv preprint arXiv:2406.02884*,  
 634 2024. 3, 7  
 635

636 Xuyong Yang, Tao Mei, Ying-Qing Xu, Yong Rui, and Shipeng Li. Automatic generation of visual-  
 637 textual presentation layout. *ACM Transactions on Multimedia Computing, Communications, and  
 638 Applications (TOMM)*, 12(2):1–22, 2016. 1  
 639

640 Ning Yu, Chia-Chih Chen, Zeyuan Chen, Rui Meng, Gang Wu, Paul Josel, Juan Carlos Niebles,  
 641 Caiming Xiong, and Ran Xu. Layoutdetr: detection transformer is a good multimodal layout  
 642 designer. In *European Conference on Computer Vision*, pp. 169–187. Springer, 2024. 3  
 643

644 Hui Zhang, Dexiang Hong, Maoke Yang, Yutao Cheng, Zhao Zhang, Jie Shao, Xinglong Wu, Zux-  
 645 uan Wu, and Yu-Gang Jiang. Creatidesign: A unified multi-conditional diffusion transformer for  
 646 creative graphic design. *arXiv preprint arXiv:2505.19114*, 2025a. 5  
 647

Jiahao Zhang, Ryota Yoshihashi, Shunsuke Kitada, Atsuki Osanai, and Yuta Nakashima.  
 Vascar: Content-aware layout generation via visual-aware self-correction. *arXiv preprint  
 arXiv:2412.04237*, 2024. 3, 6

648 Zhao Zhang, Yutao Cheng, Dexiang Hong, Maoke Yang, Gonglei Shi, Lei Ma, Hui Zhang, Jie Shao,  
649 and Xinglong Wu. Creatiposter: Towards editable and controllable multi-layer graphic design  
650 generation. *arXiv preprint arXiv:2506.10890*, 2025b. [2](#)

651

652 Xinru Zheng, Xiaotian Qiao, Ying Cao, and Rynson WH Lau. Content-aware generative modeling  
653 of graphic design layouts. *ACM Transactions on Graphics (TOG)*, 38(4):1–15, 2019. [2](#)

654

655 Yaowei Zheng, Richong Zhang, Junhao Zhang, Ye Yanhan, Ye Yanhan, and Zheyan Luo. Llamafac-  
656 tory: Unified efficient fine-tuning of 100+ language models. In *Proceedings of the 62nd Annual*  
657 *Meeting of the Association for Computational Linguistics (Volume 3: System Demonstrations)*,  
658 pp. 400–410, 2024. [8](#)

659

660 Min Zhou, Chenchen Xu, Ye Ma, Tiezheng Ge, Yuning Jiang, and Weiwei Xu. Composition-  
661 aware graphic layout gan for visual-textual presentation designs. In *Proceedings of the Thirty-*  
662 *First International Joint Conference on Artificial Intelligence*, pp. 4995–5001. International Joint  
663 Conferences on Artificial Intelligence Organization, 2022. [1](#), [2](#)

664

665

666

667

668

669

670

671

672

673

674

675

676

677

678

679

680

681

682

683

684

685

686

687

688

689

690

691

692

693

694

695

696

697

698

699

700

701